

**ACCEPTED MAY 23<sup>RD</sup> 2024**

**Mathematical modelling of Oxygen diffusion from capillary to tissues during hypoxia through multiple points using fractional balance equations with memory**

**V.Srivastava<sup>a</sup>, Dharmendra Tripathi<sup>b\*</sup>, P. K. Srivastava<sup>a</sup>, S. Kuharat<sup>c</sup> and O. Anwar Bég<sup>c</sup>**

*<sup>a</sup>Department of Applied Sciences & Humanities, Rajkiya Engineering College, Azamgarh  
[pramodpooja59@gmail.com](mailto:pramodpooja59@gmail.com)*

*<sup>b</sup>Department of Mathematics, National Institute of Technology Uttarakhand, Srinagar- 246174, India,  
[dtripathi@nituk.ac.in](mailto:dtripathi@nituk.ac.in)*

*<sup>c</sup>Multi-Physical Engineering Sciences Group, Dept. Mechanical and Aeronautical Engineering,  
Corrosion Lab, 3-08, SEE Building, Salford University, Manchester, M54WT, UK.*

*[O.A.Beg@salford.ac.uk](mailto:O.A.Beg@salford.ac.uk); [S.Kuharat2@salford.ac.uk](mailto:S.Kuharat2@salford.ac.uk)*

*\*Corresponding author E-mail: [vineetbhu@gmail.com](mailto:vineetbhu@gmail.com)*

**Abstract**

The diffusion of oxygen through capillary to surrounding tissues through multiple points along the length has been addressed in many clinical studies, largely motivated by disorders including hypoxia. However relatively few analytical or numerical studies have been communicated. In this paper, as a compliment to physiological investigations, a novel mathematical model is developed which incorporates the multiple point diffusion of oxygen from different locations in the capillary to tissues, in the form of a fractional dynamical system of equations using the concept of system of balance equations with memory. Stability analysis of the model has been conducted using the well known Routh–Hurwitz stability criterion. Comprehensive analytical solutions for the differential equation problem in the new proposed model are obtained using Henkel transformations. Both spatial and temporal variation of concentration of oxygen is visualized graphically for different control parameters. Close correlation with simpler models is achieved. Diffusion is shown to arise from different points of the capillary in decreasing order along the length of the capillary i.e. for the different values of  $z$ . The concentration magnitudes at low capillary length far exceed those further along the capillary. Furthermore with progressive distance along the capillary, the radial distance of diffusion decreases, such that oxygen diffuses only effectively in very close proximity to tissues. The simulations provide a useful benchmark for more generalized mass diffusion computations with commercial finite element and finite volume software including ANSYS FLUENT.

**Keywords:** *Fractional Diffusion Equation; Routh–Hurwitz stability criterion; Hypoxia; capillary; Henkel Transformation; mathematical biology.*

## **1. Introduction**

Capillaries are very thin and small blood vessels that connect arteries to veins and form a network throughout the body. In abnormal blood circulation, cells in the most distal region of the capillary at the venous end begin to suffer from *hypoxia* when perfusion levels (blood delivery to capillary beds in tissue) are severely reduced. Insufficient oxygen delivery to the tissues can impede metastasis and destroy part of the muscle.

Several convection and diffusion processes are involved in the systems that regulate oxygen distribution. However current understanding of the hydromechanics of these processes is still limited. Blood is oxygenated by convection, which depends on active, energy-intensive processes that create circulation flow. Diffusion transport describes the passive flow of oxygen along the concentration gradient through tissue barriers, including the alveolar capillary membrane, and between tissue capillaries and individual cells to the mitochondria in the extracellular matrix. Oxygen tension gradient, diffusion distance and tissue capillary density are all factors that affect how much diffuse oxygen moves across a given area. The rate of diffusion increases with distance and decreases with the difference between cellular and capillary oxygen concentrations [1].

In the case of hypoxia, which is a condition characterized by low oxygen levels in the body tissues, the process of oxygen diffusion from capillaries to tissues is affected. Hypoxia can occur due to various reasons, such as decreased oxygen intake, reduced blood flow, negative influence on the oxygen tension gradient, the oxygen concentration in the capillary drops too low or impaired oxygen utilization by cells.

When hypoxia, the concentration gradient of oxygen between the capillaries and the tissues is reduced, as the partial pressure of oxygen in the capillaries may also be lower. This means that the diffusion of oxygen from the capillaries to the tissues will be slower. The human body tries to compensate for hypoxia by increasing blood flow to the affected tissues. This can help to increase the oxygen delivery to the tissues and promote oxygen diffusion from the capillaries. In some cases, such as in high altitude environments (aircraft and space flight), the body can also produce more red blood cells to carry more oxygen in the bloodstream. However, in severe cases of hypoxia, the tissues may not receive enough oxygen, and this can lead to *tissue damage or even cell death*. In such cases, medical intervention may be required to improve oxygen delivery to the tissues, such as providing supplemental oxygen i.e. giving Oxygen therapy or treating the

underlying cause of hypoxia. Oxygen treatment can be quite beneficial at times, moderately beneficial at others, and virtually useless at yet other times. Thus, it is critical to comprehend the many forms of hypoxia before exploring the physiological underpinnings of oxygen treatment. In this work, among the many contributors to hypoxia we focus on a primary cause i.e. *inadequate oxygen transport to the tissues by the blood due to circulatory deficiency*.

To furnish a more accurate appraisal of the mechanisms of hypoxia or other oxygen-depletion, more sophisticated mathematical modelling can provide this facility. A mathematical model of any real-world problem provides knowledge of the problem and the ability to analyse it clearly, enables robust pragmatic solutions. A powerful methodology for improving the precision of mathematical differential equation model in medicine, is *fractional calculus*. This approach successfully generalizes the classical, integer order differential calculus to non-integer orders. In the present investigation, a fractional order differential equation is therefore applied to the modelling of oxygen diffusion from capillaries to tissues. The fractional order differential equation is particularly useful in modelling diffusion processes that exhibit anomalous behaviour, such as *long-range correlations and memory effects*, which cannot be captured by the classical diffusion equation [9, 10]. In the case of oxygen diffusion, a fractional order differential equation can be used to model the transport of oxygen molecules from the capillaries to the surrounding tissue, taking into account the spatial heterogeneity of the tissue, the oxygen consumption rate of the cells and the oxygen supply from the blood. Go [3] implemented a mathematical model for oxygen distribution through capillaries that neglected the *longitudinal diffusion of solutes in capillaries* and also assumed that the diffusion of oxygen and the oxygen consumption rate were *constant*. Diffusion processes will vary from place to place. Go [3] also noted that physical activity increases oxygen consumption rate, however it enhances the chance of certain cells to lose oxygen and influences the ability of cells engulfing capillaries to utilize or retain more oxygen than required for an additional cycle. Srivastava and Rai [4] neglected all these proposed a new mathematical model using fractional calculus. Srivastava *et al.* [5] significantly extended the work in [6] and scrutinized the effect of external forces on oxygen diffusion from capillary to tissues during hypoxia. Delgado *et al.* [7] study the fractional-order dynamics of the oxygen diffusion through capillary to tissues under the influence of external forces using a similar formulation to that developed in [4, 5] and the fractional operators of Caputo–Fabrizio. They applied the Laplace homotopy analysis method for analytical and numerical results.

Since, all biological phenomena possess memory effects from the micro level to macro level [7, 8]. Fractional calculus has been deployed very effectively to resolve challenging problems in

biomedical engineering with memory effects including corona virus transmission [9], blood coagulation [10], cancer treatment [11], biochemical enzymatic processes [12], tropical disease spread [13], ultrasonic heat transfer in tissue therapy [14], kneecap mechanics [15], corneal transplant engineering [16] and inner ear hydrodynamics [17]. Srivastava and Rai [4] used fractional order partial derivatives instead of integer order partial derivatives to explain both *sub-diffusion and diffusion processes* simultaneously to model the diffusion of oxygen in tissues through capillaries and gave approximate analytical solution using the New Iterative Method (NIM).

Since diffusion of oxygen through the capillary arises not only into the surrounding tissues, but also in the direction of the length of the capillary, this leads to a *depletion in diffusion* of oxygen into the tissues, in comparison to the net diffusion in the absence of axial diffusion along the length of the capillary. As we progress along the capillary length, the concentration of oxygen will decrease. If the length of the capillary is finite, there will be a significant difference in the concentration of oxygen at both ends but it will not be completely zero at the end [1]. At the same time, it is also important to be cognizant of the fact that diffusion/sub-diffusion of oxygen is occurring along length of the capillary, at different rates and with different concentrations, to the surrounding tissues at short axial distances [1], which cannot be explained by conventional differential diffusive models [3]. All previous formulations [3,4,5, 24, 25, 26] express the *single point diffusion at a time*, but originally the diffusion from capillary to tissues is in fact a *multiple point process*, as clearly established in [1]. To overcome this deficiency, based on the approach expounded in [11], the present investigation adopts a fractional calculus system of balance equations and develops an improved dynamical model of memory-based oxygen diffusion from capillary to tissues *not only at particular point of the capillary but also along the whole length of the capillary*.

In this paper, we model the delivery of oxygen from capillary to tissues through multipoint along its length such that the concentration of oxygen *decays gradually* [as explained in ref. [1]] using the mechanism of a memory effect based on the concept of *fractional calculus* as expressed in linear systems of balance equations. By considering a chain of balance equations, connecting each stage of concentration of oxygen to the next by means of a memory kernel, it becomes possible to derive generalised expressions for the *overall memory kernel* that connects the initial stage concentration of oxygen to the final stage concentration of oxygen. Analytical solutions are carefully derived using the well-known Henkel Transformation with physiologically robust initial

conditions and boundary conditions. Finally, a detailed elaboration on the physical implications of the solutions derived is provided.

The structure of the manuscript is as follows. Section 2 discusses the development of the proposed model for oxygen diffusion from multiple points of the capillary to surrounding tissues using a system of balance equations with memory. In Section 3, we evaluate the stability of the proposed model using Routh – Hurwitz stability criterion. In Section 4, the proposed model is solved analytically using Henkel transforms. In Section 5, we analyse and explain the results through graphs and plots. In Section 6, the paper is concluded with some discussion and glimpses of future work.

## 2. Mathematical model for oxygen diffusion from multiple points of the capillary to surrounding tissues:

In this work, we analyse the problem of hypoxia due to deficiency of oxygen transport from capillary to tissues. For the better treatment we must know the status of such deficiency, and that can be highly visualized by mathematical modelling. Now, **Fig. 1** shows the physical model of the physiological problem, where moving red blood cells in capillary diffuse the oxygen through capillary wall to surrounding tissues. In this scenario, it is quite clear that concentration of oxygen is decreased when blood is flowing along the capillary [1].

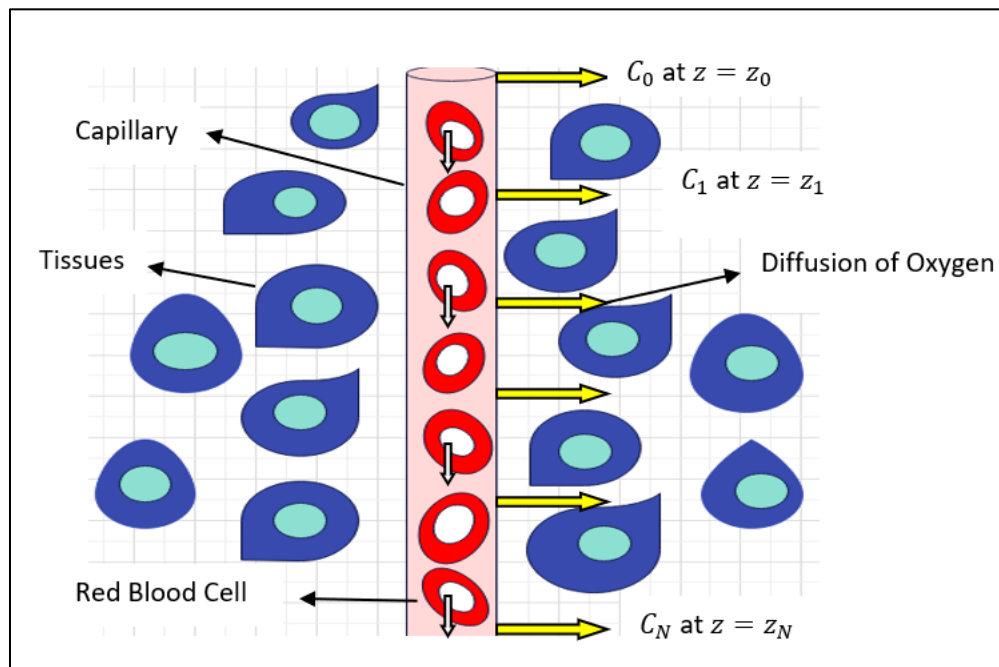


**Fig.1.** Diffusion of oxygen from multiple points to tissues through a single capillary.







Therefore, from system of equations (4), the initial values, after using convention (6), will emerge as:

$$\begin{aligned}
 U_1(r, 0) &= (e^{-z_0} - e^{-z_1}) \left( r + \frac{R^2}{r} \right) \\
 U_2(r, 0) &= (e^{-z_1} - e^{-z_2}) \left( r + \frac{R^2}{r} \right) \\
 U_3(r, 0) &= (e^{-z_2} - e^{-z_3}) \left( r + \frac{R^2}{r} \right) \\
 &\dots \dots \\
 U_N(r, 0) &= (e^{-z_{N-1}} - e^{-z_N}) \left( r + \frac{R^2}{r} \right)
 \end{aligned} \quad \dots\dots (7)$$

### 3. Stability Analysis of the Mathematical Model

In this section, the highly reliable Routh– Hurwitz stability criterion [27] is implemented to assess the numerical stability of our model. For brevity regarding the mathematical details associated with the model (1) we assume  $N = 3$ , and from equation (5) invoking convention (6) we arrive at the following system of fractional differential equations:

$$\begin{aligned}
 \frac{\partial^\alpha U_1}{\partial t^\alpha} &= d \cdot \nabla^2 U_1 - k_1 \\
 \frac{\partial^\alpha U_2}{\partial t^\alpha} &= d \cdot \nabla^2 U_2 - k_2 \\
 \frac{\partial^\alpha U_3}{\partial t^\alpha} &= d \cdot \nabla^2 U_3 - k_3 \\
 \frac{\partial^\alpha U_4}{\partial t^\alpha} &= d \cdot \nabla^2 (U_4) - k_4
 \end{aligned} \quad \dots\dots (8)$$

In Eqn. (8),  $k_4 = 0$  i.e. there is no absorption at this stage, and symmetry is assumed.

#### 3.1 Routh – Hurwitz stability criterion for fractional order system of equations[27]

Eqn. (8) can be considered as follows:

$$D^\alpha U_i = f_i(U_i).. \quad \dots\dots (9)$$

where  $f_i(U_i) = d \cdot \nabla^2 U_i - k_i$ ,  $i = 1, 2, 3, 4$ .

The associated initial conditions are:

$$\begin{aligned}
 U_1(r, 0) &= (e^{-z_0} - e^{-z_1}) \left( r + \frac{R^2}{r} \right) \\
 U_2(r, 0) &= (e^{-z_1} - e^{-z_2}) \left( r + \frac{R^2}{r} \right) \\
 U_3(r, 0) &= (e^{-z_2} - e^{-z_3}) \left( r + \frac{R^2}{r} \right)
 \end{aligned} \quad \dots \dots (10)$$

$$U_4(r, 0) = e^{-z_3} \left( r + \frac{R^2}{r} \right)$$

To determine the *critical points* of Eq. (9), we prescribe  $D^\alpha U_i = 0$ , where  $i = 1, 2, 3, 4$ . This implies that  $f_i(U_i^*) = 0$ . Let  $\zeta^*(U_1^*, U_2^*, U_3^*, U_4^*)$  be a critical point of the system (9). Now a positive term  $\delta(t)$  i.e.  $U_i = U_i^* + \delta_i(t)$  is added to the critical point for the desired perturbation. It follows that:

$$\begin{aligned} D^\alpha(U_i^* + \delta_i) &= f_i(U_i^* + \delta_i), \quad i = 1, 2, 3, 4. \\ \Rightarrow D^\alpha \delta_i &= f_i(U_i^* + \delta_i) \end{aligned} \quad \dots(11)$$

Now by Taylor's expansion we have:

$$D^\alpha \delta_i = f_i(U_i^*) + \left. \frac{\partial f_i}{\partial U_i} \right|_{eq} \delta_i + \text{higher order terms} \quad \dots(12)$$

Since  $f_i(U_i^*) = 0$ , therefore:

$$D^\alpha \delta_i \approx \left. \frac{\partial f_i}{\partial U_i} \right|_{eq} \delta_i \quad \dots (13)$$

Now, equation (13) can be derived in the form of the following matrix system:

$$D^\alpha \delta = J \delta \quad \dots(14)$$

Where  $\delta = (\delta_1, \delta_2, \delta_3, \delta_4)^T$ , and  $J(\zeta^*) = \begin{bmatrix} \frac{\partial f_1}{\partial U_1} & 0 & 0 & 0 \\ 0 & \frac{\partial f_2}{\partial U_2} & 0 & 0 \\ 0 & 0 & \frac{\partial f_3}{\partial U_3} & 0 \\ 0 & 0 & 0 & \frac{\partial f_4}{\partial U_4} \end{bmatrix}$ . Here  $J$  denotes the Jacobian

matrix computed at the critical point  $\zeta^*$ ,  $\lambda_1 = \frac{\partial f_1}{\partial U_1}$ ,  $\lambda_2 = \frac{\partial f_2}{\partial U_2}$ ,  $\lambda_3 = \frac{\partial f_3}{\partial U_3}$  and  $\lambda_4 = \frac{\partial f_4}{\partial U_4}$  are the eigenvalues of  $J$ .

The initial conditions for the system (8) are:

$$U_1(0) = U_1^* + \delta_1(0), \quad U_2(0) = U_2^* + \delta_2(0), \quad U_3(0) = U_3^* + \delta_3(0), \quad U_4(0) = U_4^* + \delta_4(0), \quad \dots(15)$$

Hence Eqn. (12) yields:

$$D^\alpha \delta_1 = \lambda_1 \delta_1, \quad D^\alpha \delta_2 = \lambda_2 \delta_2, \quad D^\alpha \delta_3 = \lambda_3 \delta_3, \quad D^\alpha \delta_4 = \lambda_4 \delta_4, \quad \dots (16)$$

The solutions of equation (16) are:

$$\delta_i(t) = E_\alpha(\lambda_i t^\alpha) \delta_i(0), \quad i = 1, 2, 3, 4. \quad \dots(17)$$

Then  $\delta_1(t), \delta_2(t), \delta_3(t), \delta_4(t)$  are decreasing. Thus the critical point  $\zeta^*$  will have local asymptotic stability if the Matignon's criterion [19] provided by  $|\arg(\lambda_i)| > \alpha \frac{\pi}{2}$  .  $i = 1, 2, 3, 4$  is fulfilled.

#### 4. Analytical solutions for the generalized multipoint diffusion model

Now applying Henkel's Transformation ( $\mathcal{H}\{C\} = \tilde{C}$ )[20] in the above system of equations (5) using the convention defined in Eqn. (6), we get:

$$\begin{array}{l}
 \text{At } z = z_0, \quad \frac{\partial^\alpha \tilde{C}_{01}}{\partial t^\alpha} = -d \cdot p^2 \tilde{C}_{01} - \frac{0.5725}{p^{1.4}} \\
 \text{At } z = z_1, \quad \frac{\partial^\alpha \tilde{C}_{12}}{\partial t^\alpha} = -d \cdot p^2 \tilde{C}_{12} - \frac{0.5725}{p^{1.4}} \\
 \text{At } z = z_2, \quad \frac{\partial^\alpha \tilde{C}_{23}}{\partial t^\alpha} = -d \cdot p^2 \tilde{C}_{23} - \frac{0.5725}{p^{1.4}} \\
 \dots \dots \dots \\
 \text{At } z = z_{m-1}, \quad \frac{\partial^\alpha \tilde{C}_{m-1 m}}{\partial t^\alpha} = -d \cdot p^2 \tilde{C}_{m-1 m} - \frac{0.5725}{p^{1.4}} \\
 \dots \dots \dots \\
 \text{At } z = z_{N-1}, \quad \frac{\partial^\alpha \tilde{C}_{N-1 N}}{\partial t^\alpha} = -d \cdot p^2 \tilde{C}_{N-1 N} - \frac{0.5725}{p^{1.4}} \\
 \text{At } z = z_N, \quad \frac{\partial^\alpha \tilde{C}_N}{\partial t^\alpha} = -d \cdot p^2 \tilde{C}_N
 \end{array} \quad \dots \dots (18)$$

In view of Matignon [19] (see Remark 7.1 in that article), the solution of the above system of equations will be:

$$\begin{array}{l}
 \tilde{C}_{01} = \tilde{C}_{01}(0)E_\alpha(-p^2 dt^\alpha) - \frac{0.57254}{p^{1.4}} \int_0^t s^{\alpha-1} E'_\alpha(-p^2 ds^\alpha) ds \\
 \tilde{C}_{12} = \tilde{C}_{12}(0)E_\alpha(-p^2 dt^\alpha) - \frac{0.57254}{p^{1.4}} \int_0^t s^{\alpha-1} E'_\alpha(-p^2 ds^\alpha) ds \\
 \tilde{C}_{23} = \tilde{C}_{23}(0)E_\alpha(-p^2 dt^\alpha) - \frac{0.57254}{p^{1.4}} \int_0^t s^{\alpha-1} E'_\alpha(-p^2 ds^\alpha) ds \\
 \dots \dots \dots \\
 \tilde{C}_{m-1 m} = \tilde{C}_{m-1 m}(0)E_\alpha(-p^2 dt^\alpha) - \frac{0.57254}{p^{1.4}} \int_0^t s^{\alpha-1} E'_\alpha(-p^2 ds^\alpha) ds \\
 \dots \dots \dots \\
 \tilde{C}_{N-1 N} = \tilde{C}_{N-1 N}(0)E_\alpha(-p^2 dt^\alpha) - \frac{0.57254}{p^{1.4}} \int_0^t s^{\alpha-1} E'_\alpha(-p^2 ds^\alpha) ds \\
 \tilde{C}_N = \tilde{C}_N(0)E_\alpha(-p^2 dt^\alpha)
 \end{array} \quad \dots \dots (19)$$

For  $N=3$  in the above system we arrive at:

$$\begin{aligned}
\tilde{C}_{01} &= \tilde{C}_{01}(0)E_\alpha(-p^2 dt^\alpha) - \frac{0.5725}{p^{1.4}} \int_0^t s^{\alpha-1} E'_\alpha(-p^2 ds^\alpha) ds \\
\tilde{C}_{12} &= \tilde{C}_{12}(0)E_\alpha(-p^2 dt^\alpha) - \frac{0.5725}{p^{1.4}} \int_0^t s^{\alpha-1} E'_\alpha(-p^2 ds^\alpha) ds \\
\tilde{C}_{23} &= \tilde{C}_{23}(0)E_\alpha(-p^2 dt^\alpha) - \frac{0.5725}{p^{1.4}} \int_0^t s^{\alpha-1} E'_\alpha(-p^2 ds^\alpha) ds \\
\tilde{C}_3 &= \tilde{C}_3(0)E_\alpha(-p^2 dt^\alpha)
\end{aligned}
\quad \Bigg| \quad \dots(20)$$

Applying the inverse Henkel Transform, ( $\mathcal{H}^{-1}\{\tilde{C}\} = C$ ), we get the following expressions:

$$\begin{aligned}
C_3(r, t) &= \mathcal{H}^{-1}\{\tilde{C}_3(p, t)\} = \mathcal{H}^{-1}\{\tilde{C}_3(p, 0)E_\alpha(-p^2 dt^\alpha)\} = e^{-z_3} \left( r + \frac{R^2}{r} + \frac{d(r^2+R^2)t^\alpha}{r^3 \Gamma[1+\alpha]} + \right. \\
&\quad \left. \frac{d^2(r^2+9R^2)t^{2\alpha}}{r^5 \Gamma[1+2\alpha]} + \frac{9d^3(r^2+25R^2)t^{3\alpha}}{r^7 \Gamma[1+3\alpha]} + \frac{225d^4(r^2+49R^2)t^{4\alpha}}{r^9 \Gamma[1+4\alpha]} \dots \dots \right) \\
&\dots(21)
\end{aligned}$$

$$\begin{aligned}
C_{23}(r, t) &= \mathcal{H}^{-1}\{\tilde{C}_{23}(p, t)\} = \mathcal{H}^{-1}\left\{\tilde{C}_{23}(p, 0)E_\alpha(-p^2 dt^\alpha) - \frac{0.5725}{p^{1.4}} \int_0^t s^{\alpha-1} E'_\alpha(-p^2 ds^\alpha) ds\right\} \\
&= (e^{-z_2} - e^{-z_3}) \left( r + \frac{R^2}{r} + \frac{d(r^2+R^2)t^\alpha}{r^3 \Gamma[1+\alpha]} + \frac{d^2(r^2+9R^2)t^{2\alpha}}{r^5 \Gamma[1+2\alpha]} + \frac{9d^3(r^2+25R^2)t^{3\alpha}}{r^7 \Gamma[1+3\alpha]} + \right. \\
&\quad \left. \frac{225d^4(r^2+49R^2)t^{4\alpha}}{r^9 \Gamma[1+4\alpha]} \dots \dots \right) - \\
&\quad \frac{0.019085 dt^{2\alpha} \left( \frac{11.5315}{r^{1.6} \Gamma[\alpha]} + dt^\alpha \left( \frac{19.6804}{r^{3.6} \Gamma[2\alpha]} + dt^\alpha \left( \frac{191.2936}{r^{5.6} \Gamma[3\alpha]} + dt^\alpha \left( \frac{4799.1733}{r^{7.6} \Gamma[4\alpha]} - \frac{231000.20958 dt^\alpha}{r^{9.6} \Gamma[5\alpha]} \right) \right) \right) \dots \right)}{\alpha^2}, \\
&\dots(22)
\end{aligned}$$

$$\begin{aligned}
C_{12}(r, t) &= \mathcal{H}^{-1}\{\tilde{C}_{12}(p, t)\} = \mathcal{H}^{-1}\left\{\tilde{C}_{12}(p, 0)E_\alpha(-p^2 dt^\alpha) - \frac{0.5725}{p^{1.4}} \int_0^t s^{\alpha-1} E'_\alpha(-p^2 ds^\alpha) ds\right\} \\
&= (e^{-z_1} - e^{-z_2}) \left( r + \frac{R^2}{r} + \frac{d(r^2+R^2)t^\alpha}{r^3 \Gamma[1+\alpha]} + \frac{d^2(r^2+9R^2)t^{2\alpha}}{r^5 \Gamma[1+2\alpha]} + \frac{9d^3(r^2+25R^2)t^{3\alpha}}{r^7 \Gamma[1+3\alpha]} + \right. \\
&\quad \left. \frac{225d^4(r^2+49R^2)t^{4\alpha}}{r^9 \Gamma[1+4\alpha]} \dots \dots \right) - \\
&\quad \frac{0.019085 dt^{2\alpha} \left( \frac{11.5315}{r^{1.6} \Gamma[\alpha]} + dt^\alpha \left( \frac{19.6804}{r^{3.6} \Gamma[2\alpha]} + dt^\alpha \left( \frac{191.2936}{r^{5.6} \Gamma[3\alpha]} + dt^\alpha \left( \frac{4799.1733}{r^{7.6} \Gamma[4\alpha]} - \frac{231000.20958 dt^\alpha}{r^{9.6} \Gamma[5\alpha]} \right) \right) \right) \dots \right)}{\alpha^2}, \\
&\dots(23)
\end{aligned}$$

$$C_{01}(r, t) = \mathcal{H}^{-1}\{\tilde{C}_{01}(p, t)\} = \mathcal{H}^{-1}\left\{\tilde{C}_{01}(p, 0)E_\alpha(-p^2 dt^\alpha) - \frac{0.5725}{p^{1.4}} \int_0^t s^{\alpha-1} E'_\alpha(-p^2 ds^\alpha) ds\right\}$$

$$\begin{aligned}
&= (e^{-z_0} - e^{-z_1}) \left( r + \frac{R^2}{r} + \frac{d(r^2+R^2)t^\alpha}{r^3\Gamma[1+\alpha]} + \frac{d^2(r^2+9R^2)t^{2\alpha}}{r^5\Gamma[1+2\alpha]} + \frac{9d^3(r^2+25R^2)t^{3\alpha}}{r^7\Gamma[1+3\alpha]} + \right. \\
&\quad \left. \frac{225d^4(r^2+49R^2)t^{4\alpha}}{r^9\Gamma[1+4\alpha]} \dots \dots \right) - \\
&\quad \frac{0.019085dt^{2\alpha} \left( -\frac{11.5315}{r^{1.6}\Gamma[\alpha]} + dt^\alpha \left( -\frac{19.6804}{r^{3.6}\Gamma[2\alpha]} + dt^\alpha \left( -\frac{191.2936}{r^{5.6}\Gamma[3\alpha]} + dt^\alpha \left( -\frac{4799.1733}{r^{7.6}\Gamma[4\alpha]} - \frac{231000.20958 dt^\alpha}{r^{9.6}\Gamma[5\alpha]} \right) \right) \right) \dots \right)}{\alpha^2}
\end{aligned} \dots(24)$$

Since  $C_{23} = C_2 - C_3$ ,  $C_{12} = C_1 - C_2$  and  $C_{01} = C_0 - C_1$ , it follows that:

$$\begin{aligned}
C_0(r, t) &= C_{01}(r, t) + C_1(r, t) \\
&= e^{-z_0} \left( r + \frac{R^2}{r} + \frac{d(r^2+R^2)t^\alpha}{r^3\Gamma[1+\alpha]} + \frac{d^2(r^2+9R^2)t^{2\alpha}}{r^5\Gamma[1+2\alpha]} + \frac{9d^3(r^2+25R^2)t^{3\alpha}}{r^7\Gamma[1+3\alpha]} + \frac{225d^4(r^2+49R^2)t^{4\alpha}}{r^9\Gamma[1+4\alpha]} \dots \dots \right) - \\
&\quad 3 * \\
&\quad \frac{0.019085dt^{2\alpha} \left( -\frac{11.5315}{r^{1.6}\Gamma[\alpha]} + dt^\alpha \left( -\frac{19.6804}{r^{3.6}\Gamma[2\alpha]} + dt^\alpha \left( -\frac{191.2936}{r^{5.6}\Gamma[3\alpha]} + dt^\alpha \left( -\frac{4799.1733}{r^{7.6}\Gamma[4\alpha]} - \frac{231000.20958 dt^\alpha}{r^{9.6}\Gamma[5\alpha]} \right) \right) \right) \dots \right)}{\alpha^2}
\end{aligned} \dots(25)$$

$$\begin{aligned}
C_1(r, t) &= C_{12}(r, t) + C_2(r, t) \\
&= e^{-z_1} \left( r + \frac{R^2}{r} + \frac{d(r^2+R^2)t^\alpha}{r^3\Gamma[1+\alpha]} + \frac{d^2(r^2+9R^2)t^{2\alpha}}{r^5\Gamma[1+2\alpha]} + \frac{9d^3(r^2+25R^2)t^{3\alpha}}{r^7\Gamma[1+3\alpha]} + \frac{225d^4(r^2+49R^2)t^{4\alpha}}{r^9\Gamma[1+4\alpha]} \dots \dots \right) - 2 * \\
&\quad \frac{0.019085dt^{2\alpha} \left( -\frac{11.5315}{r^{1.6}\Gamma[\alpha]} + dt^\alpha \left( -\frac{19.6804}{r^{3.6}\Gamma[2\alpha]} + dt^\alpha \left( -\frac{191.2936}{r^{5.6}\Gamma[3\alpha]} + dt^\alpha \left( -\frac{4799.1733}{r^{7.6}\Gamma[4\alpha]} - \frac{231000.20958 dt^\alpha}{r^{9.6}\Gamma[5\alpha]} \right) \right) \right) \dots \right)}{\alpha^2},
\end{aligned} \dots(26)$$

$$\begin{aligned}
C_2(r, t) &= C_{23}(r, t) + C_3(r, t) \\
&= e^{-z_2} \left( r + \frac{R^2}{r} + \frac{d(r^2+R^2)t^\alpha}{r^3\Gamma[1+\alpha]} + \frac{d^2(r^2+9R^2)t^{2\alpha}}{r^5\Gamma[1+2\alpha]} + \frac{9d^3(r^2+25R^2)t^{3\alpha}}{r^7\Gamma[1+3\alpha]} + \frac{225d^4(r^2+49R^2)t^{4\alpha}}{r^9\Gamma[1+4\alpha]} \dots \dots \right) - \\
&\quad \frac{0.019085dt^{2\alpha} \left( -\frac{11.5315}{r^{1.6}\Gamma[\alpha]} + dt^\alpha \left( -\frac{19.6804}{r^{3.6}\Gamma[2\alpha]} + dt^\alpha \left( -\frac{191.2936}{r^{5.6}\Gamma[3\alpha]} + dt^\alpha \left( -\frac{4799.1733}{r^{7.6}\Gamma[4\alpha]} - \frac{231000.20958 dt^\alpha}{r^{9.6}\Gamma[5\alpha]} \right) \right) \right) \dots \right)}{\alpha^2}
\end{aligned} \dots(27)$$

$$\begin{aligned}
C_3(r, t) &= e^{-z_3} \left( r + \frac{R^2}{r} + \frac{d(r^2+R^2)t^\alpha}{r^3\Gamma[1+\alpha]} + \frac{d^2(r^2+9R^2)t^{2\alpha}}{r^5\Gamma[1+2\alpha]} + \frac{9d^3(r^2+25R^2)t^{3\alpha}}{r^7\Gamma[1+3\alpha]} + \right. \\
&\quad \left. \frac{225d^4(r^2+49R^2)t^{4\alpha}}{r^9\Gamma[1+4\alpha]} \dots \dots \right)
\end{aligned} \dots(28)$$

## 5. Results and Discussion

When hypoxia is present, which can be brought on by anemia, aberrant oxygen transfer via hemoglobin, inefficient circulation, or physiological shunt, oxygen therapy has significantly less benefit since the alveoli already contain normal oxygen levels. Instead, the issue is a deficiency in one or more of the systems that carry oxygen from the lungs to the tissues. Nevertheless, even if the amount carried by hemoglobin is rarely changed, a tiny amount of excess oxygen, between 7 and 30 percent, can be transported in the dissolved state in the blood when alveolar oxygen is raised to the maximum. This fractional quantity of excess oxygen may constitute the difference between life and death [2]. It has been established in previous sections, that through refined mathematical models (Eqn. 1) one can easily determine the approximate position of highly effected regions. The analytical solutions derived in section 4 have been numerically computed using symbolic software, Mathematica 11.3 (Wolfram Research, <https://www.wolfram.com/mathematica/new-in-11/>). All data utilized for the graphical plots given in this section is based on physiologically robust sources [19, 20]. Comparing Fig.3 of ref. [4] to Fig 2, evidently similar topologies are computed indicating that there is a significant variation of concentration of oxygen with respect to a change in the order of derivative ( $\alpha$ ), at  $z = 0.1$  and  $r = 0.1$ . From this, it is clear that we remodelled the original problem, as described in ref. [1, 4] without changing its originality. An additional advantage of our model is that diffusion is more precisely simulated from different points of the capillary in decreasing order along the length of the capillary i.e. for the different values of  $z$ , the values of  $C_0(r, t)$ ,  $C_1(r, t)$ ,  $C_2(r, t)$  and  $C_3(r, t)$  are demonstrably depleted as witnessed in **Fig.3** at same time, which concurs with actual physiological observations [1]. It is important to note that very shallow gradients of concentration with respect to time are computed at low values of ( $\alpha$ ). The growth rate of oxygen diffusion is therefore low for this scenario. However as ( $\alpha$ ) is elevated a very strong enhancement in temporal concentration gradient is induced and this further is amplified at greater time values.

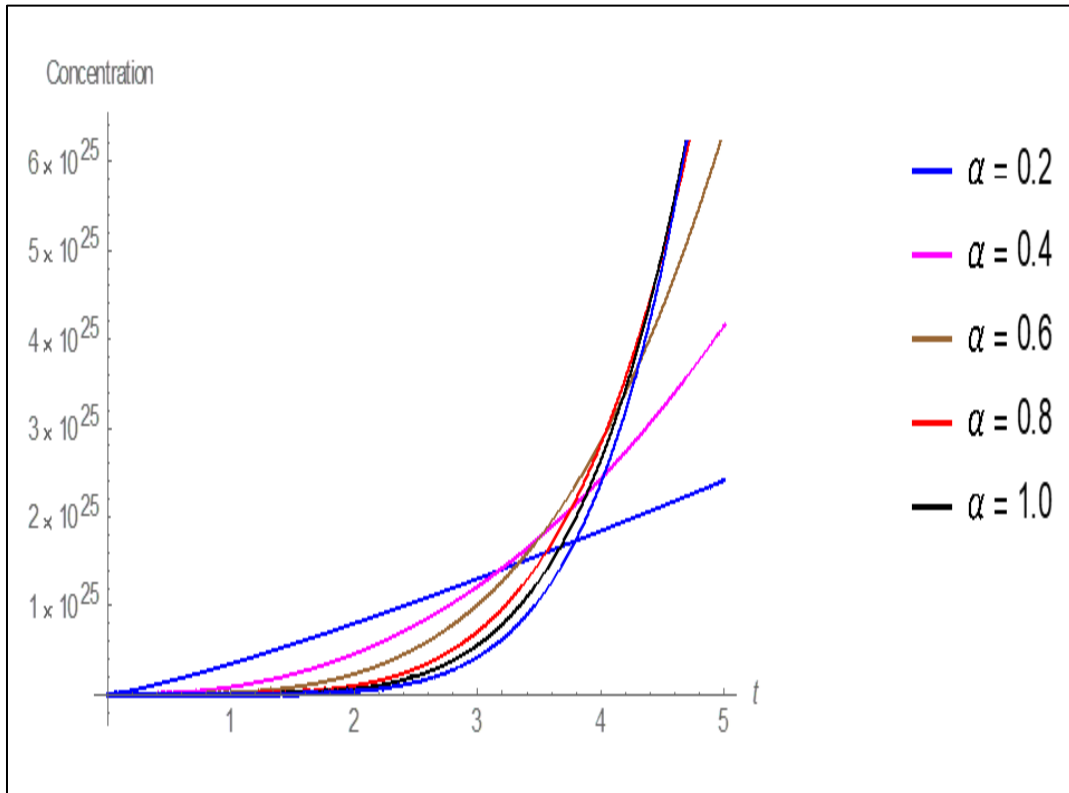


**Fig. 2.** Variation of concentration of oxygen versus time with respect to change in  $\alpha$ , at  $z = 0.1, r = 0.1, d = 1.0, R = 0.0001$ .

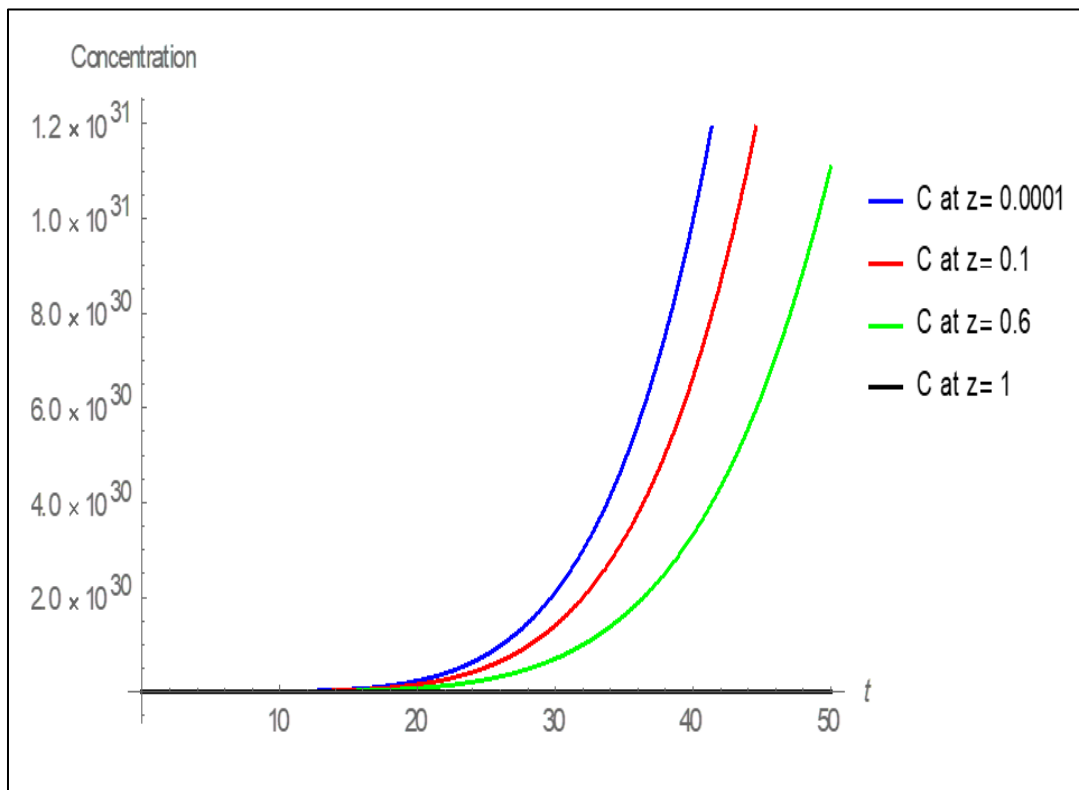


**Fig. 3.** Concentration of Oxygen versus time  $t$  with  $\alpha = 0.9; d = 1; R = 0.0001; at r = 0.01$ .

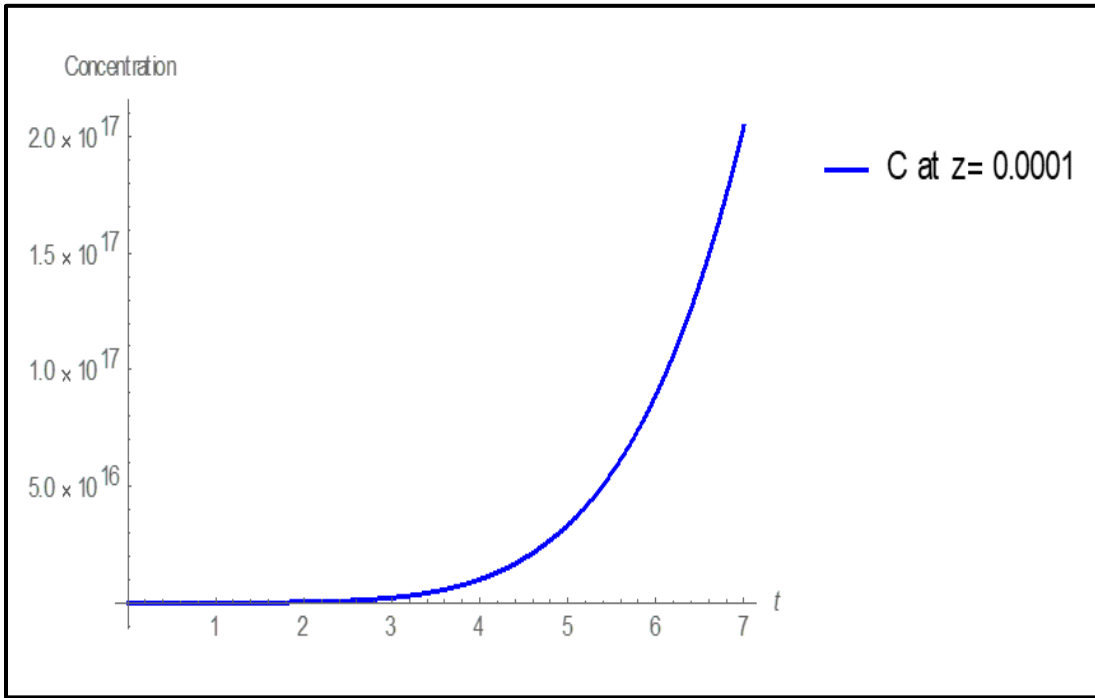


**Fig. 4.** Concentration of Oxygen versus time  $t$  with  $\alpha = 0.9$ ;  $d = 1$ ;  $R = 0.0001$ ; at  $r = 0.01$ .

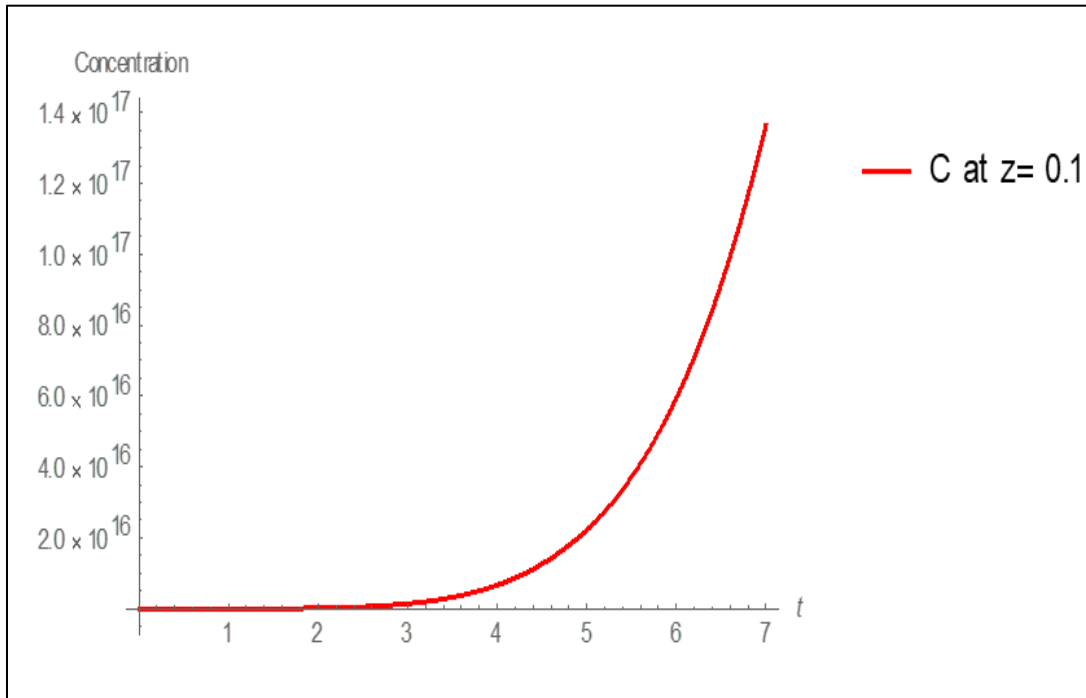


**Fig. 5.** Concentration of Oxygen versus time  $t$  with  $\alpha = 0.9$ ;  $d = 1$ ;  $R = 0.0001$ ; at  $r = 0.01$ .

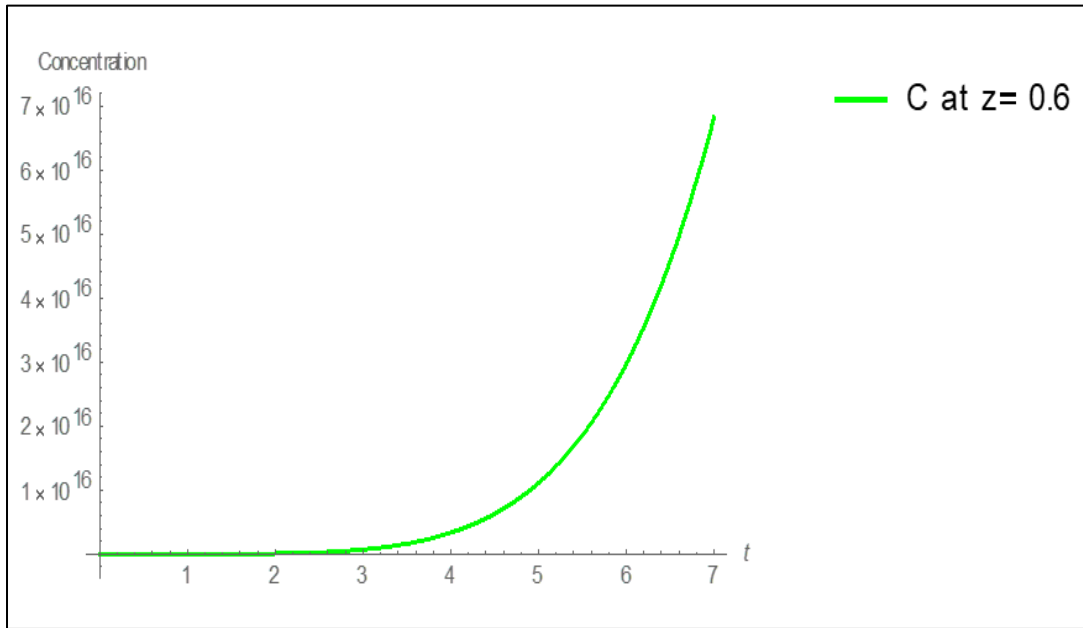


**Fig. 6.**Concentration of Oxygen versus time  $t$  with  $\alpha = 0.9$ ;  $d = 1$ ;  $R = 0.0001$ ; at  $r = 0.01$ .

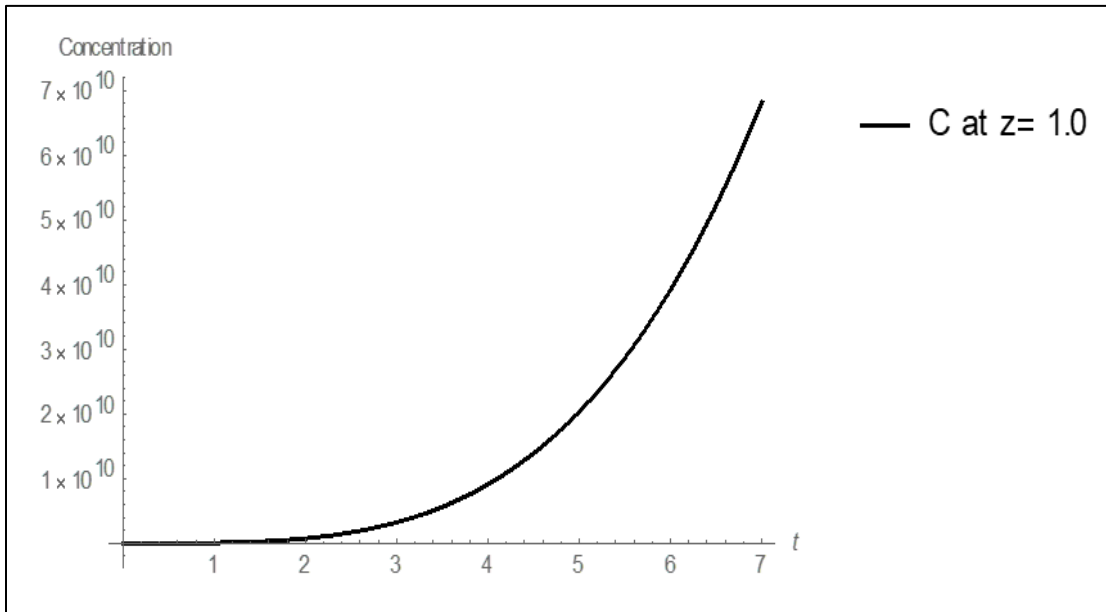


**Fig. 7.**Concentration of Oxygen versus time  $t$  with  $\alpha = 0.9$ ;  $d = 1$ ;  $R = 0.0001$ ; at  $r = 0.01$ .

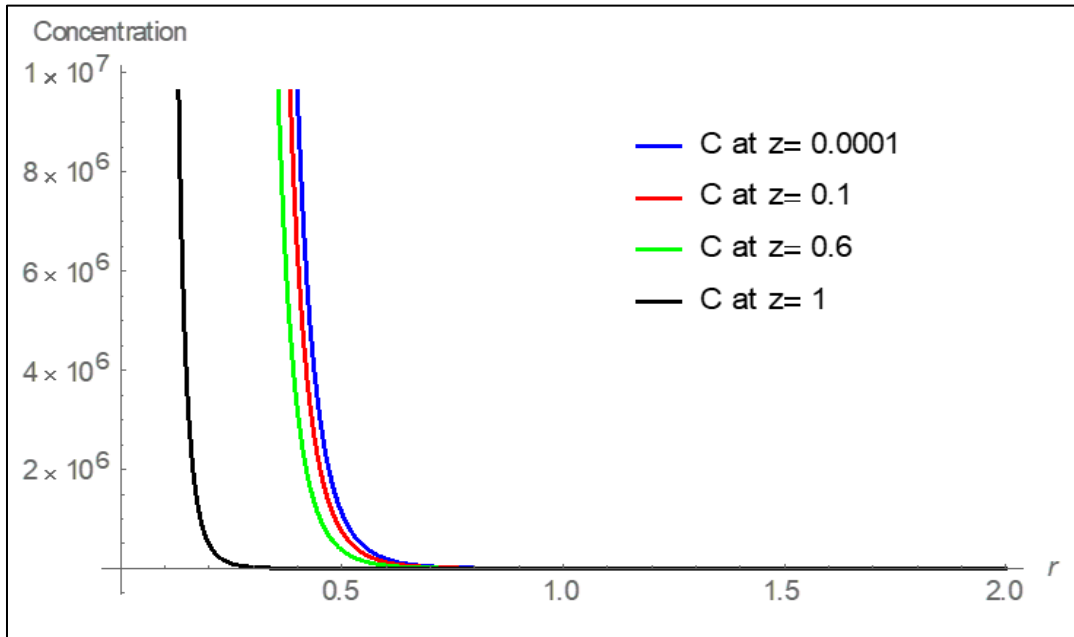


**Fig. 8.** Variation of concentration of Oxygen with *radial direction*  $r$  for  $\alpha = 0.9$ ;  $d = 1$ ;  $R = 0.0001$ ; at  $t = 1$ .

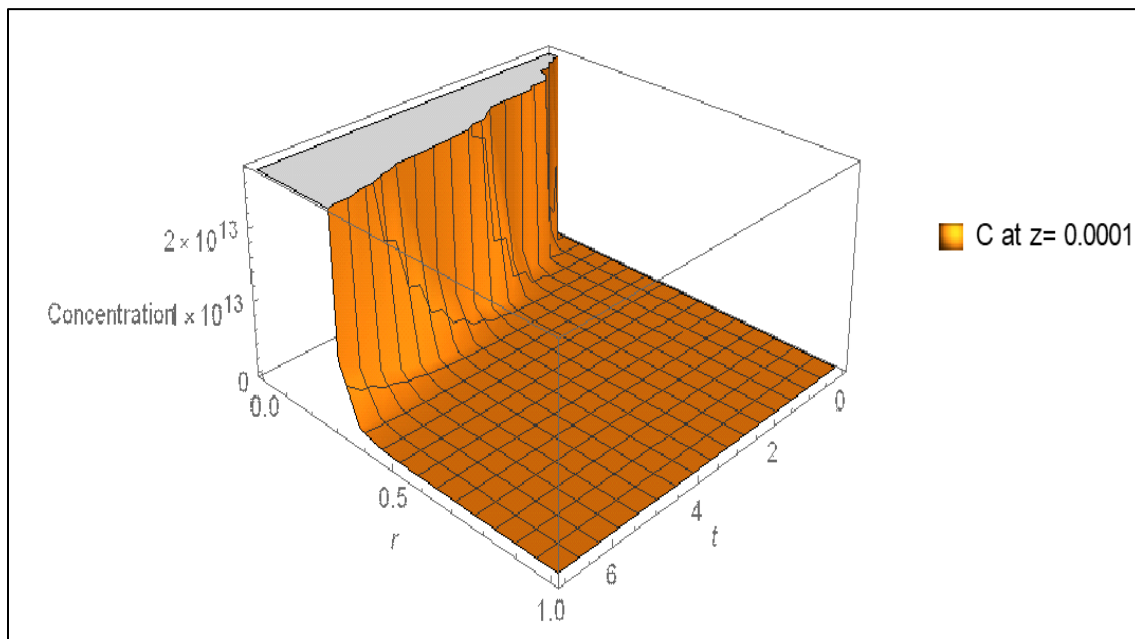


**Fig. 9.** Variation of concentration of Oxygen with *radial direction*  $r$  and *time*  $t$  for  $\alpha = 0.9$ ;  $d = 1$ ;  $R = 0.0001$ .

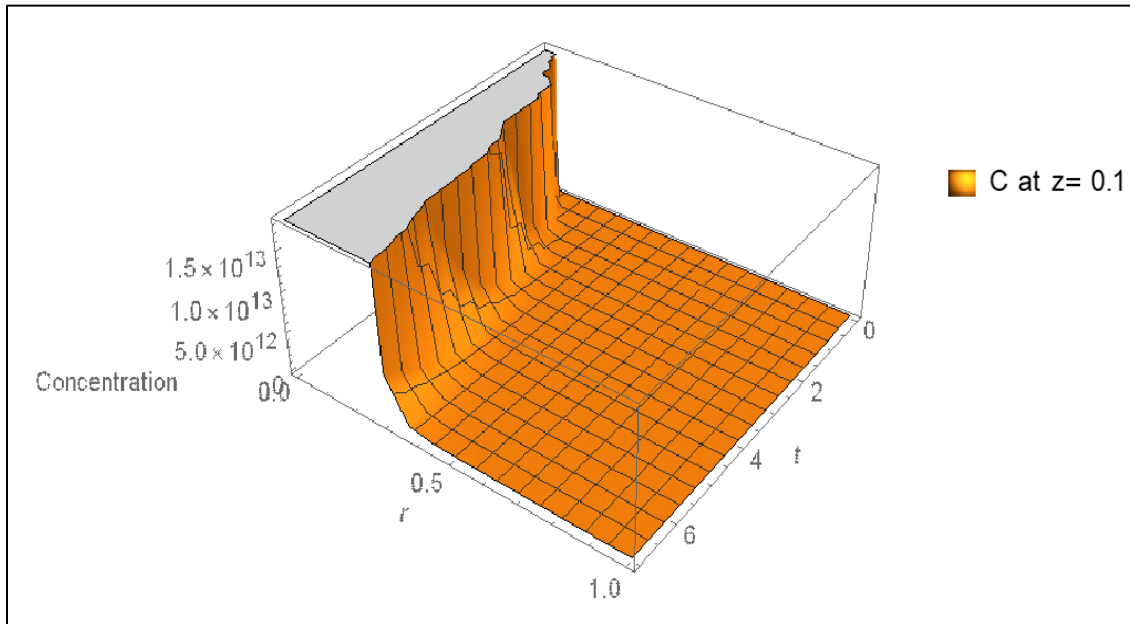


**Fig. 10.** Variation of concentration of Oxygen with radial direction  $r$  and time  $t$  for  $\alpha = 0.9$ ;  $d = 1$ ;  $R = 0.0001$ .

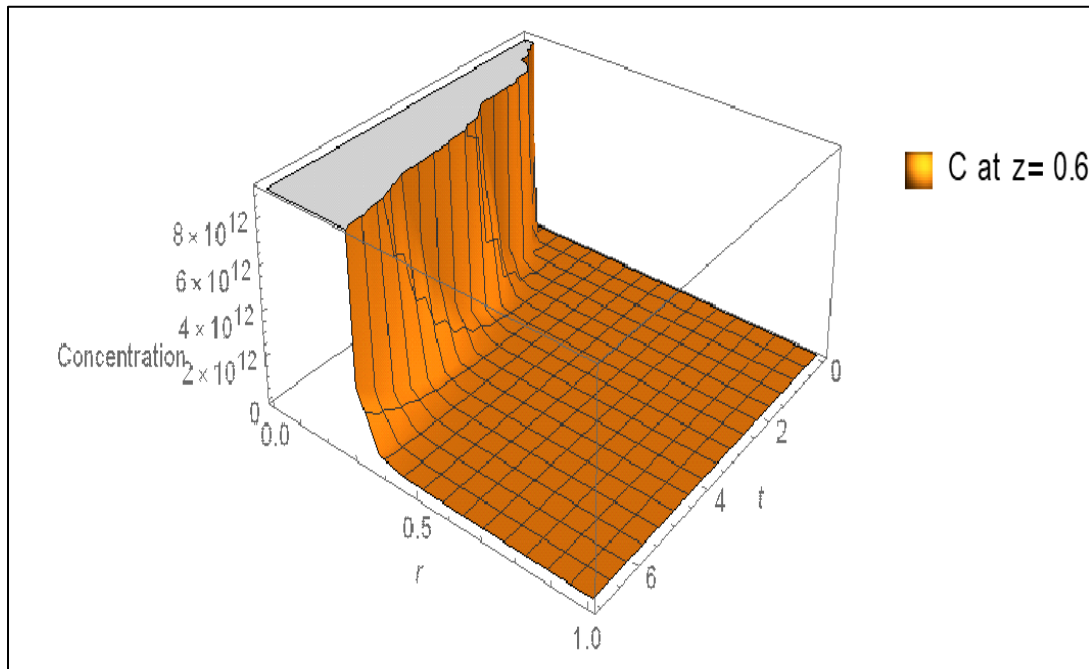


**Fig. 11.** Variation of Concentration of Oxygen with *radial direction*  $r$  and *time*  $t$  for  $\alpha = 0.9$ ;  $d = 1$ ;  $R = 0.0001$ .

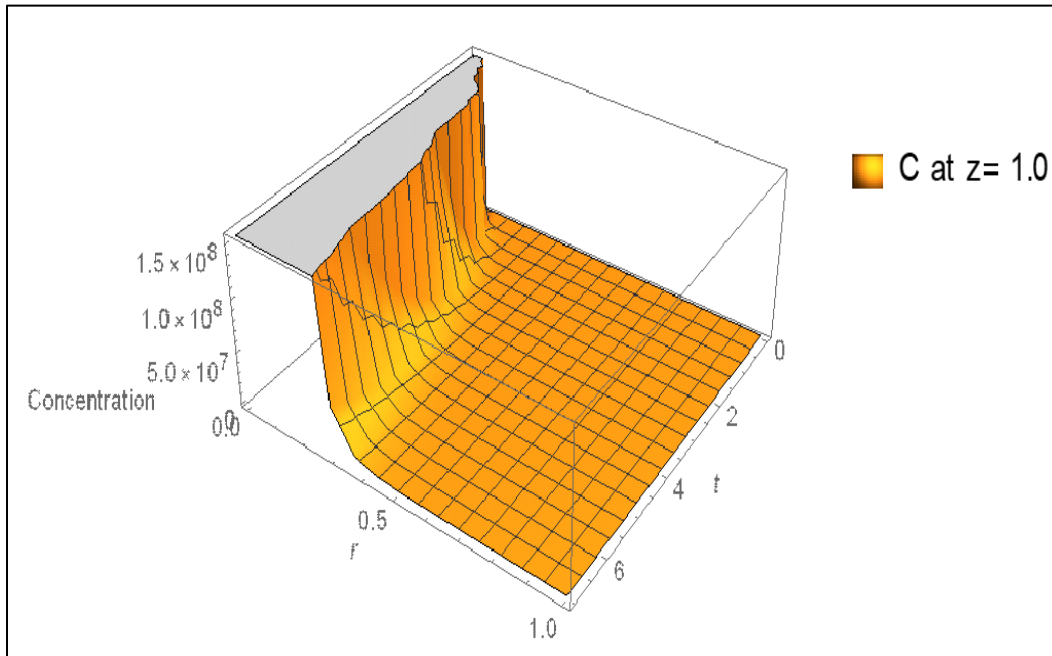


**Fig. 12.** Variation of concentration of Oxygen with *radial direction r* and *time t* for  $\alpha = 0.9$ ;  $d = 1$ ;  $R = 0.0001$ .

To clarify this more accurately **Fig.4, Fig.5, Fig.6, Fig.7** are displayed. It is apparent from inspection of these plots that the concentration of oxygen at  $z = 0.0001$  is much greater than the concentration of oxygen at  $z = 1.0$  (compare fig 4 and 5). In both these plots, concentration remains invariant with time up to  $t \sim 3$ , thereafter there is a very sharp ascent in concentration. The diffusion process is therefore amplified both at short axial distances and large time elapse whereas it is suppressed at longer axial distance and low time values. **Figs 6 and 7** clearly demonstrate that as  $z$  is increased to 0.6 and the maximum value of 1 (termination of the capillary), the oxygen concentration magnitude reduces by an order of magnitude (from  $10^{17}$  to  $10^{16}$ ) and eventually is massively depleted by many orders of magnitude to  $10^{10}$ . The topologies of the plots however remain consistent with invariance at small times and rapid ascents at larger times. Also this pattern is further emphasized in **Fig.8**, where as one moves along the length of the capillary the radial distance of diffusion decreases. Therefore the oxygen diffuses only in the zones of tissues which are very close to the capillary due to the decrease in concentration of oxygen along the capillary length. Furthermore asymptotic decays are computed in oxygen concentration with radial distance which is very distinct from the monotonic ascents computed in earlier figures with time. Peak concentrations, in consistency with physiological experiments, always arise near the centre of the capillary ( $r = 0$ ) and minimal magnitudes are generated at large radial distances (periphery of the capillary,  $r = 2$ ). The strong dependence of the diffusion process on time i.e. unsteady phenomena is clearly captured. **In Fig.9 to Fig.12**, the variations of concentration of oxygen with respect to

radial coordinate  $r$  and time  $t$  are visualized simultaneously at the locations,  $z = 0.0001, 0.1, 0.6$  and  $1.0$  respectively. These contour plots confirm that maximum oxygen concentrations consistently arise at low radial coordinate values and high values of time, irrespective of the variation in other parameters.

## 6. Conclusions

A comprehensive fractional differential mathematical model for Oxygen diffusion from capillary to tissues during hypoxia with memory has been developed for *multiple points*, generalizing previous studies which were restricted to *single point* diffusion [4], with effect of external force [5]. The diffusion of oxygen through capillary to surrounding tissues through multiple points has been reported in previous studies, but it has not been considered in mathematical models. This concept of multiple point detection simultaneously will greatly assist in a more robust clinical approach and subsequent therapies for hypoxia. As we have highlighted above, a very small amount of extra oxygen may create the big difference in therapy, if one is able to correctly identify the most appropriate region. The present study proposed for the first time therefore a theoretical fluid dynamics model that incorporates the multiple point diffusion of oxygen from different locations along the capillary length to tissues in the form of a fractional dynamical system of equations. A special case of this generalized model is retrieved for single point diffusion and agrees exactly with the formulation in [4]. A numerical stability analysis of the dynamical model utilizing the Routh – Hurwitz stability criterion has also been conducted. Thereafter analytical solutions of the proposed model have been derived with Henkel transforms applied to the conventional model (using  $\alpha_0 = \alpha_1 = \alpha_2 = \dots \alpha_n = \alpha$ ). Physiologically realistic scenarios have been simulated. Both spatial and temporal variation of concentration of oxygen is visualized graphically for different control parameters. All numerical computation have been done using symbolic software, Mathematica 11.3. The main findings of the present analysis can be summarized as follows:

- a) Improved accuracy is achieved with the new generalized multipoint model compared with the classical single point model.
- b) Close correlation with simpler models is achieved.
- c) Diffusion is shown to arise from different points of the capillary in decreasing order along the length of the capillary i.e. for the different values of  $z$ .
- d) The concentration magnitudes at low capillary length far exceed those further along the capillary.

- e) With progressive distance along the capillary, the radial distance of diffusion decreases, such that oxygen diffuses only effectively in very close proximity to tissues.
- f) The concentration exhibits a monotonic ascent in time whereas it decays asymptotically with radial coordinate.

The simulations provide a useful benchmark for more generalized mass diffusion computations with complex oxygen gradients and partial pressures with commercial finite element and finite volume software including ANSYS FLUENT, ADINA-F, STAR-C, CFD-ACE etc. Future studies may therefore utilize fully 3-D convective-diffusive models and also consider Taylor hydrodynamic dispersion. An additional pathway may be to explore the use of nanoparticles to enhance diffusion of oxygen with consideration of thermal convection in heat conducting blood flows in capillaries.

### **Acknowledgments**

The authors are grateful to both reviewers for their comments which have served to improve the clarity of the article.

### **References:**

- [1] R.M. Leach, D.F. Treacher, ABC of oxygen. Oxygen transport-2. Tissue hypoxia, *Clinical Rev. BMJ* 317 (1998) 1370–1373.
- [2] A. C. Guyton, J. E. Hall, *Textbook of Medical Physiology*, 11<sup>th</sup> Edition, Saunders, Elsevier, INDIA (2007).
- [3] JaeGwi Go, Oxygen delivery through capillaries, *Math. Biosci.* 208 (2007) 166–176.
- [4] V. Srivastava, K.N. Rai, A multi-term fractional diffusion equation for oxygen delivery through a capillary to tissues. *Mathematical and Computer Modelling* 51 (2010) 616–624.
- [5] V. Srivastava, D. Tripathi and O. Anwar Bég, Numerical study of oxygen diffusion from capillary to tissues during hypoxia with external force effects, *Journal of Mechanics in Medicine and Biology*, Vol. 17, No. 2 (2016) 1750027 (20 pages).
- [6] V.F. Morales-Delgado, J.F. Gómez-Aguilar, Khaled M. Saad, Muhammad Altaf Khan, P. Agarwal, Analytic solution for oxygen diffusion from capillary to tissues involving external force effects: A fractional calculus approach, *Physica A*, 523 (2019) 48–65.
- [7] Dobrescu R, Purcarea VL, Emergence, self-organization and morphogenesis in biological structures, *Journal of Medicine and Life* Vol. 4, No.1, 2011, pp.82-90.
- [8] Sally C. Pias, How does oxygen diffuse from capillaries to tissue mitochondria? Barriers and pathways, *Journal of Physiology* 599.6 (2021) pp 1769-1782.

- [9] Laécio Carvalho de Barros, Michele Martins Lopes, Francielle Santo Pedro, Estevão Esmi, José Paulo Carvalho dos Santos and Daniel Eduardo Sánchez, The memory effect on fractional calculus: an application in the spread of COVID-19, *Computational and Applied Mathematics* (2021) 40:72 pp 1-21.
- [10] C. Ionescu, A. Lopes, D. Copot, J.A.T. Machado, J.H.T. Bates, The role of fractional calculus in modelling biological phenomena: A review, *Communications in Nonlinear Science and Numerical Simulation*, 51, 2017, Pages 141-159.
- [11] T. A-Poiana *et al.*, Fractional calculus in mathematical oncology, *Sci Rep.* 2023; 13: 10083.
- [12] Dulf EH, Vodnar DC, Danku A, Muresan CI, Crisan O. Fractional-order models for biochemical processes. *Fractal Fract.* 2020; 4(2):12.
- [13] Veerasha P, Akinyemi L, Oluwasegun K, Şenol M, Oduro B. Numerical surfaces of fractional Zika virus model with diffusion effect of mosquito-borne and sexually transmitted disease. *Math. Methods Appl. Sci.* 2022;45(5):2994–3013.
- [14] A. F. Elsayed and O. Anwar Bég, New computational approaches for biophysical heat transfer in tissue under ultrasonic waves: Variational iteration and Chebyshev spectral simulations, *J. Mechanics Medicine Biology*, 14, 3, 1450043.1-1450043.17 (17 pages) (2014). DOI: 10.1142/S0219519414500432
- [15] P. A. Smyth and I. Green, Fractional calculus model of articular cartilage based on experimental stress-relaxation, *Mechanics of Time-Dependent Materials*, 19, pages 209–228 (2015).
- [16] D. Mandal *et al.*, Constitutive modelling of human cornea through fractional calculus approach, *Physics of Fluids* 35, 031907 (2023).
- [17] Nemanja I. Kovincic & Dragan T. Spasicodynamics of a middle ear with fractional type of dissipation, *Nonlinear Dynamics*, 85, 2369–2388 (2016).
- [18] R. Nigmatullin, D. Baleanu, A. Fernandez, Balance equations with generalised memory and the emerging fractional kernels, *Nonlinear Dynamics*, 104, pages 4149–4161 (2021).
- [19] D. Matignon, Stability results for fractional differential equations with applications to control processing, In. *Comput. Eng. Syst. Appl. IIMACS, 2. IEEE-SMC*; 1996. P 963-8.
- [20] E. Kreyszig, *Advanced Engineering Mathematics*, 10<sup>th</sup> Edn, Wiley, USA (2015).
- [21] K. Diethelm, *The Analysis of Fractional Differential Equations*, Springer, Berlin, 2010.
- [22] K. Diethelm, N. J. Ford, Multi-order fractional differential equations and their numerical solution, *Applied Mathematics and Computation*, 154 (2004) 621–640.

- [23] Amy G. Tsai, Paul C. Johnson, and Marcos Intaglietta, Oxygen gradients in the microcirculation, *Physiol Rev*, 83: 933–963, 2003.
- [24] Adrien Lücker, Bruno Weber, and Patrick Jenny, A dynamic model of oxygen transport from capillaries to tissue with moving red blood cells, *Am J Physiol Heart Circ Physiol* 308: H206–H216, 2015.
- [25] Kovtanyuk A, Chebotarev A and Lampe R, Mathematical modelling of cerebral oxygen transport from capillaries to tissue. *Front. Appl. Math. Stat.* 9:1257066 (2023)
- [26] Andrey E. Kovtanyuk , Alexander Yu. Chebotarev, Nikolai D. Botkin, Varvara L. Turova, Irina N. Sidorenko , and Renée Lampe, Nonstationary model of oxygen transport in brain tissue, *Computational and Mathematical Methods in Medicine*, Volume 2020, Article ID 4861654, 9 pages.
- [27] S. Bourafa, M-S. Abdelouahab, A. Moussaoui, On some extended Routh–Hurwitz conditions for fractional-order autonomous systems of order  $\alpha \in (0, 2)$  and their applications to some population dynamic models, *Chaos, Solitons and Fractals*, 133 (2020), 109623.